Journal of Magnetism and Magnetic Materials 420 (2016) 23–27

Contents lists available at ScienceDirect

Journal of Magnetism and Magnetic Materials

journal homepage: www.elsevier.com/locate/jmmm

Microwave absorption of electroplated NiFeCu/Cu multilayers deposited directly on Si (100) substrates

B.G. Silva, D.E. Gonzalez-Chavez, J. Gomes Filho, R.L. Sommer *

Centro Brasileiro de Pesquisas Físicas, 22290-180 Rio de Janeiro, RJ, Brazil

ARTICLE INFO

Article history:
Received 22 March 2016
Received in revised form
20 May 2016
Accepted 25 June 2016
Available online 28 June 2016

Keywords:
Electroplating
NiFeCu/Cu multilayers
Broadband FMR
Dynamic anisotropy
Rotatable anisotropy

ABSTRACT

We study the magnetic properties and broadband microwave absorption of electroplated NiFeCu/Cu multilayered thin films deposited directly on Si (100) substrates. We produced samples with 20 nm thick NiFeCu layers and Cu layer thickness t_{Cu} in the range 0–2.8 nm. Structural properties were studied by grazing incidence X-ray diffraction (GIXRD), while the composition and morphological aspects were studied by scanning electron microscopy (SEM) and energy dispersive X-ray spectroscopy (EDX). GIXRD confirmed the cubic face centered FCC phase of NiFeCu with all diffraction peaks drifting toward lower angles with t_{Cu}. SEM images show the appearance of Cu islands instead of continuous Cu layers. A minimum coercive field of 1.4 Oe is obtained for t_{Cu} = 1.0 nm, while the ferromagnetic resonance linewidth exhibited 200 Oe constant values for t_{Cu} between 0.7 and 2.1 nm. The effective magnetization increases with t_{Cu}, possibly associated to the increase on Fe content as observed by EDX. The effective dynamic anisotropy behavior with t_{Cu} seems to be associated to the island structure observed in the films.

1. Introduction

Permalloy and its alloys are widely used materials for magnetic and magneto-electronic devices operating from DC to microwave frequencies. For these devices, multilayered films of NiFe alloys are usually produced using sophisticated and expensive high vacuum techniques. They allow a good control of the layer interfaces and the stress level inside the films, resulting in a very good control of the magnetic anisotropies, microwave absorption and damping. A very well known material produced with these methods is NiFe/Cu multilayers, which exhibit high magnetoimpedance ratio [1–3], magnetoresistance [4,5] and good microwave frequency response [6].

An alternate method to fabricate nanostructured NiFe based materials is electroplating, which is a very high throughput technique. Besides it presents low implementation and operation costs. However, owed to its nature, the main mechanisms of film growth in electrodeposition are different from high vacuum techniques. In particular, parameters such as electrolyte pH, concentration, deposition potentials, additives, substrates, besides deposition modes (galvanostatic or potentiostatic) substantially affect the properties of film deposits. One drawback is that when using solutions for NiFe and Cu layer depositions it is virtually impossible to deposit NiFe without a given amount of Cu, due the codeposition of the more noble metal (Cu) during the deposition of the less noble component (NiFe). As a consequence most of the reported results in the literature mention NiFeCu/Cu multilayered films [7–11]. Early reports show improved magnetic properties for nominally thin layers with no detailed microstructural analyses [7,8]. More recently, Tokarz et al. [9] and Esmaili et al. [10] reported well defined electroplated NiFeCu/Cu multilayers for tens of nanometers layer thickness. While for few nanometers Cu layers no clear NiFeCu/Cu interfaces were reported [9].

Ferromagnetic resonance studies were carried out in electroplated FeCo, FeCoNi films and CoCu/Cu as well as NiCu/Cu multilayers, showing in general high damping and large FMR-linewidth [12–15].

In this work, we study the microwave absorption of electroplated NiFeCu/Cu multilayered thin films with fixed thickness of NiFeCu (t=20 nm) and varying copper layer thickness t_{Cu} = 0–2.8 nm. The dispersion relation, linewidth, DC magnetic properties are investigated as a function of the Cu layer thickness, nominal compositions and morphological and microstructural aspects of the films.

2. Experimental

Multilayered NiFeCu/Cu films were grown by electrodeposition on (100) n-doped Si substrates with nominal resistivity 5–10 Ω cm at room temperature. The samples were fabricated, without

* Corresponding author.
E-mail address: sommer@cbpf.br (R.L. Sommer).

http://dx.doi.org/10.1016/j.jmmm.2016.06.076
0304-8853/

stirring, using a three-electrode electrochemical cell. The silicon substrates were firstly cleaned in a diluted HCl aqueous solution and rinsed in bi-distilled water just before the deposition. The working electrodes were prepared by attaching the unpolished side of the substrates on a stainless steel rod with a GaIn contact. For the deposition, the whole electrode was covered with chemical resisting tape, leaving a exposed circular region (area = 0.2463 cm^2) on the polished side of the substrates. The counter electrode was made of a spiral Pt wire and a Ag/AgCl (3M KCl) reference electrode was used. The depositions were controlled by an AUTOLAB – PGSTAT 30 POTENTIOSTAT working in potentiostatic mode. The electrolyte solution was based on the previous work of Quemper et al. [16]. It was prepared with Milli-Q™ water using a diluted solution of H_2SO_4 to adjust pH to 3.4. A small (10 mM) quantity of $CuSO_4$ was added in order to introduce Cu^{+2} ions in the electrolyte. The NiFeCu deposition process was done at −1.10 V which resulted the lowest coercive field for a 150 nm thick film. The nominal layer thickness was estimated from the deposited charge in all cases, based on Faraday's law. Copper layers were deposited at −0.55 V following the copper reduction peak as seen in the measured voltammogram of the electrolyte (not shown).

Multilayered samples ([NiFeCu/Cu] ×50) were produced with NiFeCu nominal thickness fixed at 20 nm, while the copper nominal thickness (t_{Cu}) was varied from 0.4 to 2.8 nm. A sample without copper layers ($t_{Cu} = 0$) was also produced.

Structural properties were investigated with X-ray diffraction using a Panalytical X'Pert Pro diffractometer with CuK_α radiation ($\lambda = 1.54056$ Å). The grazing incidence technique (GIXRD) at a fixed angle of 1.5° was used in order to reduce the influence of the substrate in the diffraction patterns.

Scanning electron microscopy (SEM) and energy dispersive X-ray spectroscopy (EDX) were used for imaging and compositional studies, respectively.

Static hysteresis loops (M vs. H) were obtained with an alternating gradient field magnetometer (AGFM) under a dc magnetic field H in the range ±600 Oe.

Microwave absorption was studied with a broadband ferromagnetic resonance setup composed of a Rohde and Schwarz ZVA24 vector network analyzer combined with a coplanar waveguide (CPW) with a 260 μm wide central conductor. During these measurements the sample was placed on top of the CPW which generates a radio frequency field h_{rf} oriented mostly in the plane of the sample and perpendicular to the propagation direction of the CPW.

An in-plane dc magnetic field in the range of ±1000 Oe was applied perpendicularly ($H \perp h_{rf}$) in order to obtain the ferromagnetic resonance spectra (magnetic absorption) for frequencies in the range of 0.5–12.0 GHz following the procedure described in Gonzalez- Chavez et al. [17] where additional details of the VNA-FMR setup can also be found.

3. Results and discussion

In Fig. 1 GIXRD diffraction spectra of selected NiFeCu/Cu films are presented. The patterns show intense peaks of the NiFeCu FCC phase at $2\theta \approx 44.2°$ (111), indicating this preferential texture for all studied samples. There were also peaks at $2\theta \approx 51.5°$ (200), $2\theta \approx 76.0°$ (220), $2\theta \approx 92.2°$ (311) and $2\theta \approx 97.8°$ (222). Other peaks are originated from substrate and sample holder.

A shift to lower angles is observed for all peaks with increasing copper layer thickness, as shown in Fig. 2. This indicates that some of the copper migrates into the NiFeCu layer during the deposition of the copper layers as already reported in Ghosh et al. [18].

The linewidth of the NiFeCu (111) diffraction peaks was obtained by fitting the experimental diffraction lines with a Voigt function. The Full Width at Half Maximum (FWHM) as function of copper layer thickness is shown in Fig. 3. From this figure it can be observed that linewidth increases linearly with the copper thickness. This can be attributed to the effect of the strain in the NiFeCu phase, either originated from the NiFeCu/Cu interface or from the NiFeCu layer itself.

SEM images (shown in Fig. 4) reveal that for all samples with copper layers, isolated copper islands do appear on film surfaces show up, suggesting a Volmer–Weber growth mode of Cu, while the pure NiFeCu film exhibits a smooth surface. This behavior is

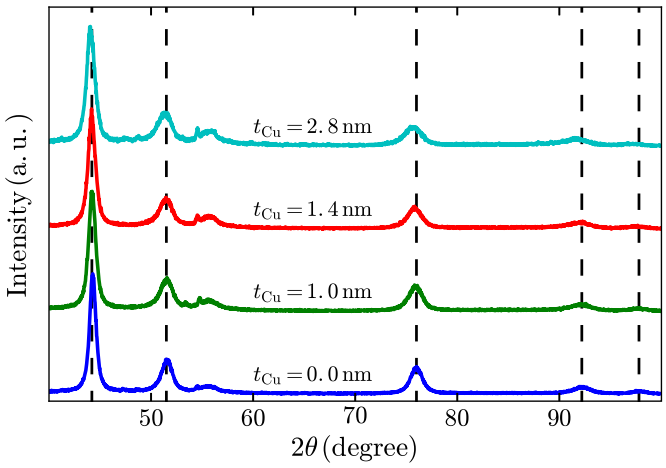

Fig. 1. X-ray diffraction patterns (grazing incidence) for selected samples with increasing copper layer thickness.

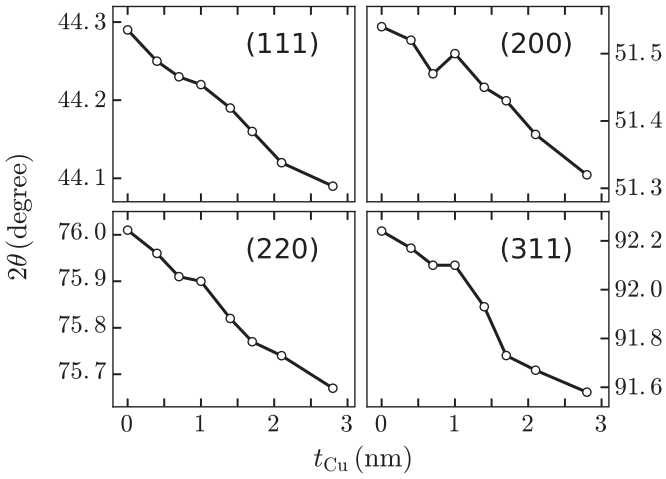

Fig. 2. NiFeCu peaks displacement as a function of copper layer thickness.

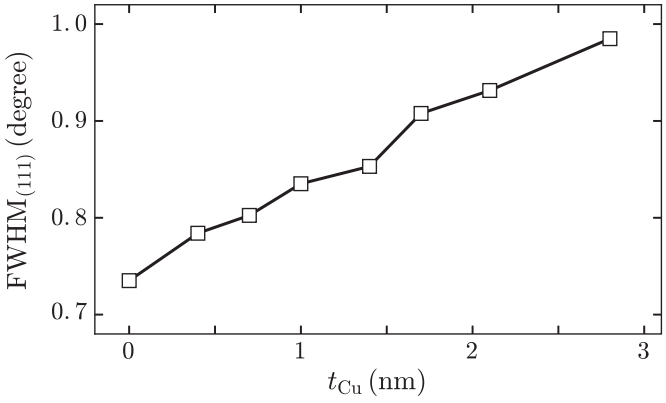

Fig. 3. NiFeCu (111) linewidth evolution as a function of copper layer thickness.

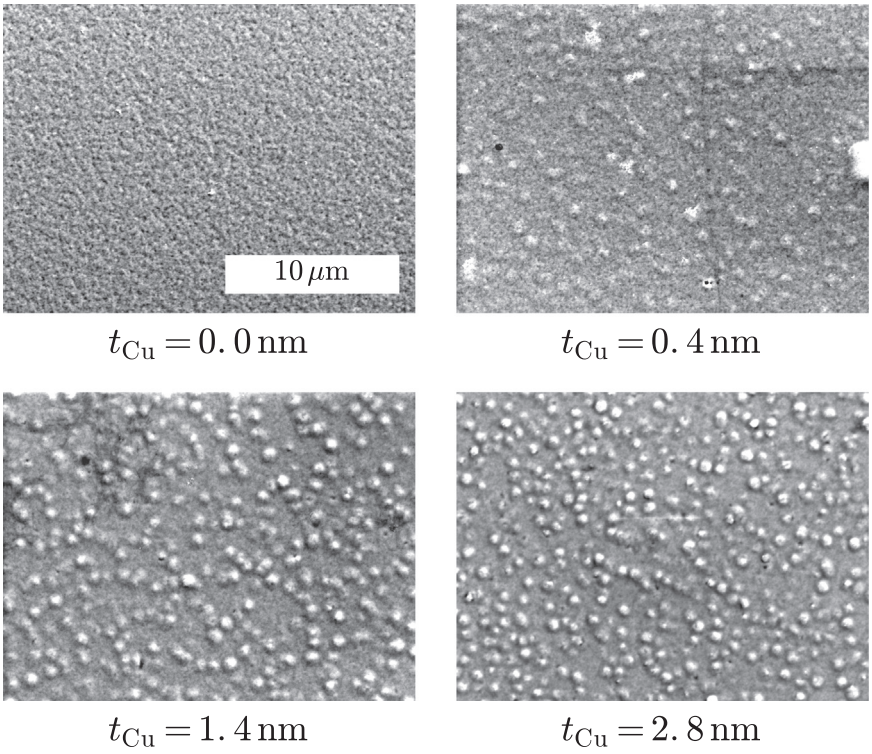

Fig. 4. SEM images for electroplated samples on Si substrate: (a) Pure NiFeCu (t=1000 nm), (b) NiFeCu/Cu multilayers for t_{Cu} = 0.4 nm, (c) t_{Cu} = 1.4 nm and (d) t_{Cu} = 2.8 nm.

also observed in samples with reduced number of layers (not shown). An EDX analysis on the islands showed that they are mainly composed by copper, while the rest of the film surface is the NiFeCu phase.

On the other hand, EDX also showed that the composition of the NiFeCu phase changes: Fe and Cu content increases while the Ni content decreases with t_{Cu} (see Fig. 5). These results indicate that RX linewidth broadening is owed to the strain of NiFeCu phase originated at the interface with the copper islands. Statistical analysis on the density of islands per area and island sizes reveals an increase of the density of islands with copper thickness, while the size distributions showed a mean island size around 750 nm and low dispersion for all samples.

The static hysteresis loops (M vs. H) measured along the parallel (0°) and transverse (90°) directions of the samples are shown in Fig. 6. The (0°) was defined according the position of each sample in the sample holder. From the shapes and coercive fields on both directions no noticeable in plane anisotropy was observed for all samples.

Coercive field (H_c) for the sample without copper layer is

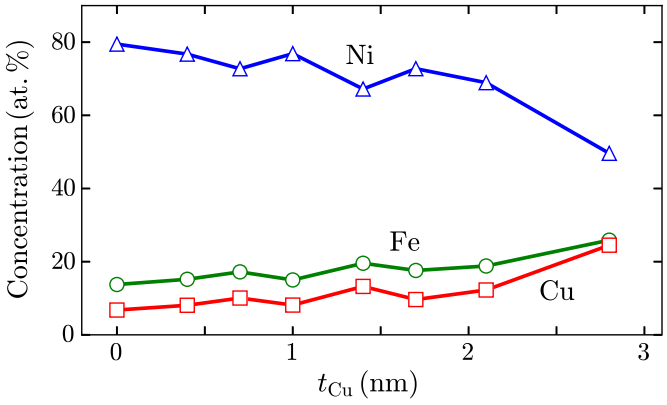

Fig. 5. Ni, Fe and Cu atomic percent content as a function of copper thickness.

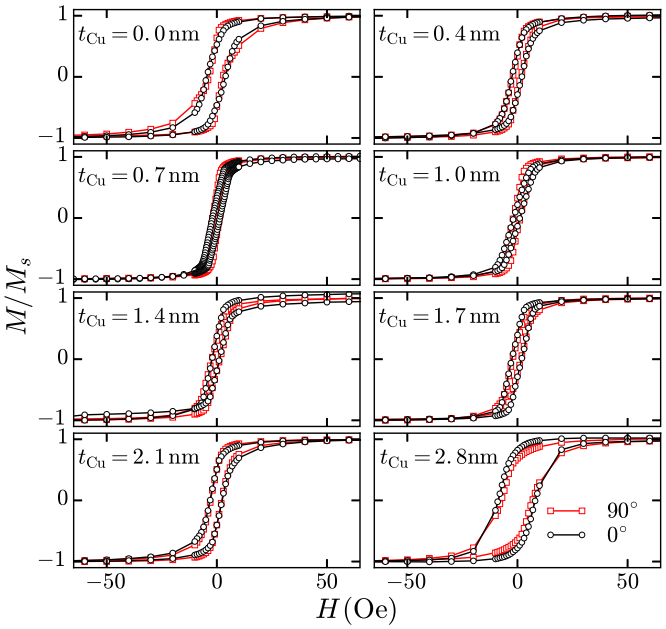

Fig. 6. Magnetization curves for all samples measured at 0° (black lines) and 90° (red lines). (For interpretation of the references to color in this figure caption, the reader is referred to the web version of this paper.)

3.2 Oe. For the multilayered samples the H_c decreases, except for the sample with t_{Cu} = 2.8 nm with H_c=7.1 Oe. A minimum of H_c=1.4 Oe is observed for t_{Cu}=1.0 nm as shown in Fig. 7.

Fig. 8 shows measured FMR absorption spectra for selected samples. No appreciable changes were observed for measurements at 0° or 90° of the same sample. The color scale denotes the absorption amplitude.

The amplitude maxima on the branches correspond to the resonant modes which define the dispersion relation (resonant frequency f_r vs. applied field H) shown in Fig. 9.

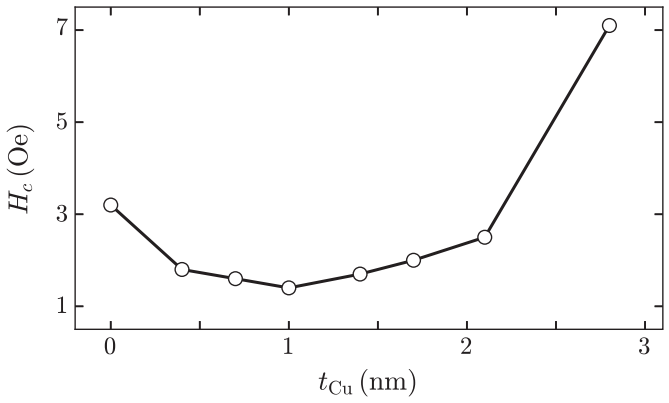

Fig. 7. Coercive field for 0° as a function of copper thickness. The minimum H_c=1.4 Oe was obtained for t_{Cu} = 1 nm.

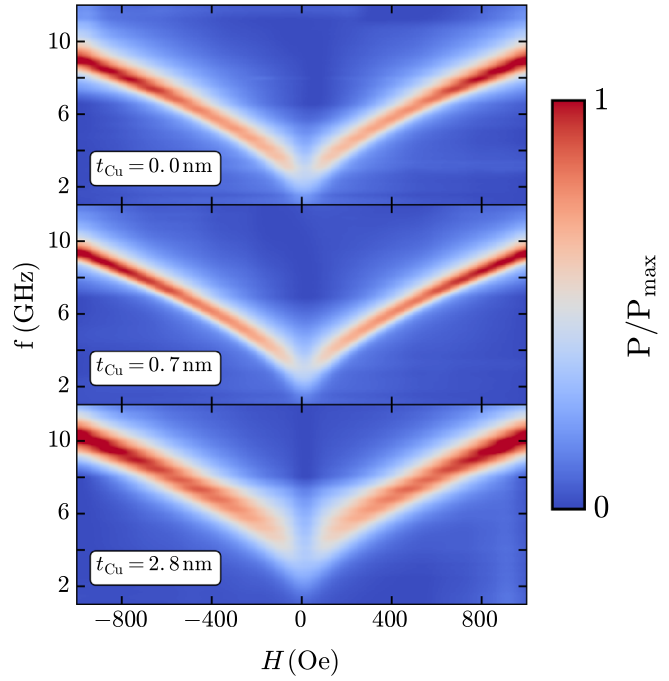

Fig. 8. Experimental microwave absorption spectra for selected samples.

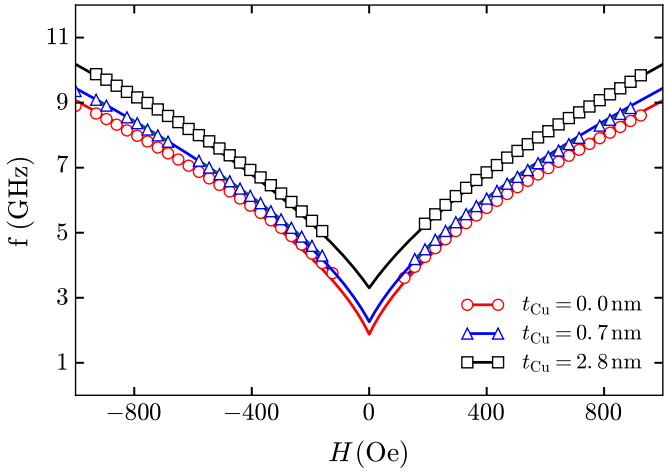

Fig. 9. Dispersion relations for the spectra shown in Fig. 8. Symbols are experimental data; solid lines are fittings to Kittel formula.

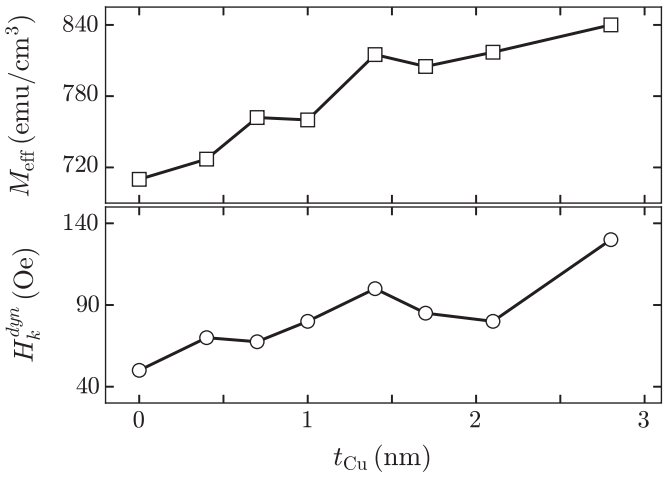

Fig. 10. Effective magnetization M_{eff} and anisotropy field $H_k{}^{dyn}$ as a function of copper thickness. The values were obtained from fittings with Kittel formula.

From these figures it can be noticed that with increasing t_{Cu} the dispersion relations shift toward higher frequencies. Also an appreciable change in the resonance linewidth (width of the branches) is observed. In order to quantify these behaviors we fit the experimental dispersion relations using the Kittel formula

$$2\pi f_r = \gamma\sqrt{(4\pi M_{eff} + H + H_k^{dyn})(H + H_k^{dyn})} \quad (1)$$

where M_{eff} is the effective magnetization, $H_k{}^{dyn}$ is the effective dynamic anisotropy field and γ = 17.6 MHz/Oe. The obtained fitted parameters, M_{eff} and $H_k{}^{dyn}$, are shown in Fig. 10 where we observe a large increase of $H_k{}^{dyn}$ and a moderate but clear increase of M_{eff} with larger t_{Cu}.

We must emphasise that $H_k{}^{dyn}$ is not related to an in-plane uniaxial anisotropy as our samples shows no experimental differences for M vs. H or FMR absorption measurements at 0° and 90°. Rather $H_k{}^{dyn}$ is owed to micromagnetic features that in the Kittel model behave as a rotatable anisotropy [19–22], which means that the anisotropy axis follows the magnetization direction. The experimental effect of this kind of anisotropy is the frequency shift in the dispersion relations, as observed in Fig. 9. To understand the physical origin of this effect, one has to consider that the copper islands will create large distortions on the local fields due local dynamic demagnetizing effects even though the dispersion relations are obtained for saturated samples. These distortions are possibly the origin of the measured $H_k{}^{dyn}$ which increases with increasing t_{Cu}.

The increase of M_{eff} is reflected as a larger slope on the dispersion relations as function of t_{Cu}. When compared to the EDX analyses it becomes clear that the increase of M_{eff} with t_{Cu} is related to the corresponding larger contend of Fe in the NiFeCu film.

The linewidth was measured as full height mean width of the resonant peaks at 8.0 GHz fitted with a Lorentzian function. The results are shown in Fig. 11. From this figure we observe that the film without copper layers have a linewidth of 273 Oe which is large when compared to sputtered films as usual, owed to electrodeposition process [23]. This linewidth could be attributed to large magnetic anisotropy dispersions inside the film, which could also explains the large $H_k{}^{dyn}$ (50 Oe). On the other hand, the copper layers make linewidth larger for t_{Cu} = 0.4 nm, while for samples with t_{Cu} between 0.7 and 2.1 nm, linewidth is reduced to about 200 Oe remains almost constant.

It must be noticed that, even if the copper layers are not continuous, we expect that a copper rich interface between successive NiFeCu layer is formed. This will decrease linewidth and coercive field due to stress relief, with a clear exception for t_{Cu} = 2.8 nm. For this last sample the stoichiometry of the Ni(49.6)Fe(25.9)Cu(24.5)

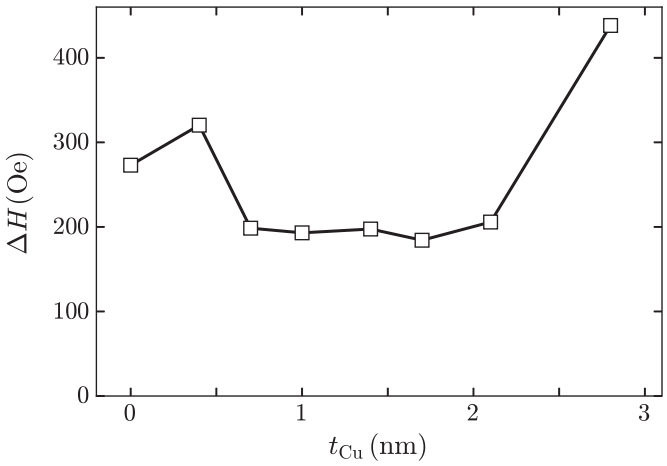

Fig. 11. FMR-linewidth as a function of copper layer thickness.

is already entering in the range of ($\gamma_1 + \gamma_2$) phase with a high change of precipitation and magnetic hardening [24]. The slight linewidth increase for the $t_{Cu} = 0.4$ nm sample can be possibly attributed to not clear interfaces between NiFeCu layers due to low copper content.

4. Conclusions

We studied the microwave absorption properties of NiFeCu/Cu multilayers directly deposited on n-type Si (100) as function of the Cu layer thickness. All samples presented small values of coercive field with exception of the sample with $t_{Cu} = 2.8$ nm which is already entering in the range of ($\gamma_1 + \gamma_2$) phase. FMR-linewidths at 8.0 GHz were around 200 Oe, mainly due to the Cu island structure effect on the anisotropy dispersion. The Cu layer thickness was observed to affect the overall stoichiometry of all layers, changing the effective magnetization and the effective dynamic anisotropy.

Acknowledgment

This work has been supported by the Brazilian agencies CNPq, FAPERJ and CAPES.

References

[1] L. Panina, K. Mohri, Magneto-impedance in multilayer films, Sens. Actuators A: Phys. 81 (1) (2000) 71–77.
[2] G. Kurlyandskaya, L. Elbaile, F. Alves, B. Ahamada, R. Barrue, A. Svalov, V. VasKovskiy, Domain structure and magnetization process of a giant magnetoimpedance geometry FeNi/Cu/FeNi (Cu) FeNi/Cu/FeNi sensitive element, J. Phys.: Condens. Matter 16 (36) (2004) 6561.
[3] A. de Andrade, M.A. Corrêa, A. Viegas, F. Bohn, R.L. Sommer, Magnetization dynamics in nanostructures with weak/strong anisotropy, J. Appl. Phys. 115 (10) (2014) 103908.
[4] B. Dieny, V.S. Speriosu, S.S. Parkin, B.A. Gurney, D.R. Wilhoit, D. Mauri, Giant magnetoresistive in soft ferromagnetic multilayers, Phys. Rev. B 43 (1) (1991) 1297.
[5] P. Holody, W. Chiang, R. Loloee, J. Bass, W. Pratt Jr, P. Schroeder, Giant magnetoresistance of copper/permalloy multilayers, Phys. Rev. B 58 (18) (1998) 12230.
[6] J. Dubowik, F. Stobiecki, T. Luciński, Interface magnetism in permalloy/Cu multilayers: ferromagnetic-resonance study, Phys. Rev. B 57 (10) (1998) 5955.
[7] K. Attenborough, R. Hart, S.J. Lane, M. Alper, W. Schwarzacher, Magnetoresistance in electrodeposited Ni-Fe-Cu/Cu multilayers, J. Magn. Magn. Mater. 148 (1) (1995) 335–336.
[8] E. Chassaing, P. Nallet, M. Trichet, Electrodeposition of Cu/Fe20Ni80 magnetic multilayers, J. Electrochem. Soc. 143 (5) (1996) L98–L100.
[9] A. Tokarz, P. Wieczorek, A. Lis, J. Morgiel, Microstructure of electrodeposited NiFe/Cu multilayers, J. Microsc. 237 (3) (2010) 456–460.
[10] S. Esmaili, M. Bahrololoom, L. Péter, Magnetoresistance of electrodeposited NiFeCu alloys, Thin Solid Films 520 (6) (2012) 2190–2194.
[11] H. Kuru, H. Kockar, M. Alper, Electrodeposited NiFeCu/Cu multilayers: effect of Fe ion concentration on properties, J. Magn. Magn. Mater. 373 (2015) 135–139.
[12] D. Zhou, M. Zhou, M. Zhu, X. Yang, M. Yue, Electrodeposition and magnetic properties of FeCo alloy films, J. Appl. Phys. 111 (7) (2012) 07A319.
[13] M. Dariel, L. Bennett, D. Lashmore, P. Lubitz, M. Rubinstein, W. Lechter, M. Harford, Properties of electrodeposited Co-Cu multilayer structures, J. Appl. Phys. 61 (8) (1987) 4067–4069.
[14] H. Lassri, H. Ouahmane, H. El Fanity, M. Bouanani, F. Cherkaoui, A. Berrada, Ferromagnetic resonance studies of electrodeposited Ni/Cu multilayers, Thin Solid Films 389 (1) (2001) 245–249.
[15] X. Liu, J.O. Rantschler, C. Alexander, G. Zangari, High-frequency behavior of electrodeposited Fe-Co-Ni alloys, IEEE Trans. Magn. 39 (5) (2003) 2362–2364.
[16] J.-M. Quemper, S. Nicolas, J. Gilles, J. Grandchamp, A. Bosseboeuf, T. Bourouina, E. Dufour-Gergam, Permalloy electroplating through photoresist molds, Sens. Actuators A: Phys. 74 (1) (1999) 1–4.
[17] D. Gonzalez-Chavez, R. Dutra, W. Rosa, T. Marcondes, A. Mello, R. Sommer, Interlayer coupling in spin valves studied by broadband ferromagnetic resonance, Phys. Rev. B 88 (10) (2013) 104431.
[18] S. Ghosh, S. Singh, S. Basu, Structural and magnetic characterization of electrodeposited Ni/Cu multilayers, Mater. Chem. Phys. 120 (1) (2010) 199–205.
[19] J.B. Youssef, N. Vukadinovic, D. Billet, M. Labrune, Thickness-dependent magnetic excitations in permalloy films with nonuniform magnetization, Phys. Rev. B 69 (17) (2004) 174402.
[20] M. Schneider, A. Kos, T. Silva, Dynamic anisotropy of thin permalloy films measured by use of angle-resolved pulsed inductive microwave magnetometry, Appl. Phys. Lett. 86 (20) (2005) 202503.
[21] L. Phua, N. Phuoc, C. Ong, Investigation of the microstructure, magnetic and microwave properties of electrodeposited NixFe1 − x (x=0.2 − 0.76) films, J. Alloys Compd. 520 (2012) 132–139.
[22] W.T. Soh, N.N. Phuoc, C. Tan, C. Ong, Magnetization dynamics in permalloy films with stripe domains, J. Appl. Phys. 114 (5) (2013) 053908.
[23] M.D. De Sihues, C. Durante-Rincón, J. Fermin, A ferromagnetic resonance study of NiFe alloy thin films, J. Magn. Magn. Mater. 316 (2) (2007) e462–e465.
[24] R.M. Bozorth, Ferromagnetism, Wiley-IEEE, New York, 1993.